Journal of Medicinal Chemistry Article

J. Med. Chem. **2010,** *53,* 7521–7531 **7521**
DOI: 10.1021/jm100387d

Selection of Evodiamine as a Novel Topoisomerase I Inhibitor by Structure-Based Virtual Screening and Hit Optimization of Evodiamine Derivatives as Antitumor Agents

Guoqiang Dong,[†] Chunquan Sheng,*[,†] Shengzheng Wang, Zhenyuan Miao, Jianzhong Yao, and Wannian Zhang*

Department of Medicinal Chemistry, School of Pharmacy, Second Military Medical University, 325 Guohe Road, Shanghai 200433, People's Republic of China. [†]*These two authors contributed equally to this work.*

Received March 27, 2010

Human topoisomerase I (TopoI) is recognized as a valuable target for the development of effective antitumor agents. Structure-based virtual screening was applied to the discovery of structurally diverse TopoI inhibitors. From 23 compounds selected by virtual screening, a total of 14 compounds were found to be TopoI inhibitors. Five hits (compounds **1**, **14**, **20**, **21**, and **23**) also showed moderate to good in vitro antitumor activity. These novel structures can be considered as good starting points for the development of new antitumor lead compounds. Hit **20** (evodiamine) was chosen for preliminary structure−activity relationship studies. Various groups, including alkyl, benzoyl, benzyl and ester, were introduced to the indole nitrogen atom of evodiamine. The substituted benzoyl groups were found to be favorable for the antitumor activity and spectrum. The 4-Cl benzoyl derivative, compound **29u**, was the most active one with IC_{50} values in the range 0.049−2.6 μM.

Introduction

DNA topoisomerase I (TopoI[a]) is a ubiquitous and essential enzyme in mammals.[1] TopoI produces a single strand break in DNA allowing relaxation of DNA supercoils. The catalytic mechanism involves a nucleophilic attack by the active site tyrosine OH group (Tyr723 in human TopoI) on the phosphate group at 3′-end of the cutting strand,[2] which results in the broken of the DNA phosphodiester bond and the formation of a binary DNA−TopoI covalent complex (cleavable complex). After cleavage, the broken (scissile) DNA strand can rotate around the unbroken (nonscissile) strand and remove DNA supercoils.

TopoI is a validated target for cancer chemotherapy[3] since its identification as the only target of camptothecin (CPT),[4] which was first isolated from the Chinese tree *Camptotheca acuminata* by Wall and co-workers in 1966.[5] CPT and its derivatives act by binding to a transient TopoI−DNA covalent complex, leading to an accumulation of DNA strand breaks upon replication, ultimately resulting in cell death during the S phase of the cell cycle.[6−8] CPT shows potent antitumor activity and has been evaluated in the clinic. However, its therapeutic application is hindered because of poor aqueous solubility and high in vivo hepatoxicity. Subsequently, the structural modification of natural CPT has generated many new CPT derivatives with improved pharmacological or pharmacokinetic profile.[9−11] For example, topotecan[12] and irinotecan[13] (Figure 1) have entered clinical use. Several drug candidates, such as rubitecan,[14] lurtotecan,[15] and exatecan,[16] are currently at different stages of the clinical trials.

Although CPT analogues have achieved great success in clinical cancer chemotherapy, the intrinsic instability of the highly electrophilic α-hydroxylactone of the E ring undergoes rapid hydrolysis to the biologically inactive carboxylate form under physiological conditions.[17] In order to improve the stability of E-ring, two kinds of modifications have been performed. One approach is the insertion of a methylene spacer between the alcohol and carboxyl functions of CPT to obtain homocamptothecin (hCPT).[18] The modified A and/or B ring hCPT analogues[19−22] have produced two candidates in clinical trial (i.e., diflomotecan[23] and BN80927,[24] Figure 1). The second approach is the conversion of the E-ring to a five-membered ring (α-keto derivatives).[25] They can completely block E-ring-opening and retain high TopoI inhibitory activity. The cyclobutane methylenedioxy derivative S39625 (Figure 1) shows remarkable potency and is under consideration for clinical trials.[26]

Although CPT derivatives are the only clinically approved TopoI inhibitors, they have several major limitations:[1,3,27,28] (1) As discussed above, CPTs are chemically unstable and rapidly inactivated to carboxylate in blood;. (2) The CPT-trapped cleavage complexes reverse within minutes after drug removal,[29] which means that they must be given as prolonged and/or repeated infusions to maintain persistent cleavage complexes. (3) Cells overexpressing the drug efflux membrane transporters are cross-resistant to CPTs.[30−32] Moreover, several resistance mutations of TopoI (such as Asn722S and Arg364H) have been reported.[33,34] (4) The side effects of camptothecins are dose-limiting and potentially severe (such as diarrhea and neutropenia), which limit the dose that can be safely administered.

To overcome the drawbacks of CPTs, the discovery of non-CPT TopoI inhibitors has recently emerged as a promising field to find better antitumor agents. Among non-CPT compounds, the most promising are indolocarbazoles, indenoisoquinolines,

*To whom correspondence should be addressed. For C.S.: phone/fax, 86-21-65516994; e-mail, shengcq@hotmail.com. For W.Z.: phone/fax, 86-21-81871243; e-mail, zhangwnk@hotmail.com.

[a] Abbreviations: TopoI, topoisomerase I; CPT, camptothecin; hCPT, homocamptothecin; SBVS, structure-based virtual screening; rmsd, root-mean-square deviation; SAR, structure−activity relationship; MD, molecular dynamics; GA, genetic algorithm; OD, absorbance.

Published on Web 10/13/2010

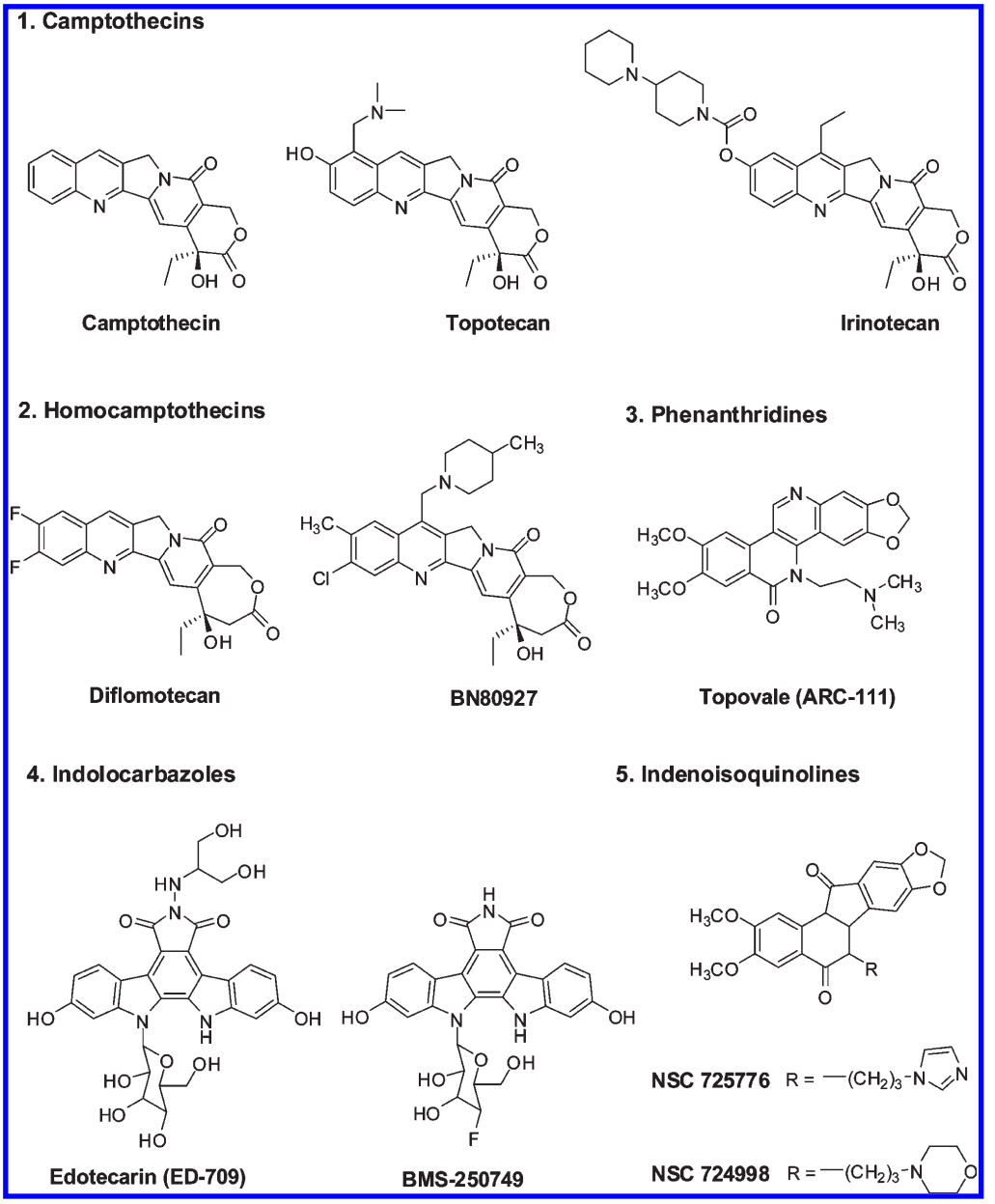

Figure 1. Chemical structures of clinical relevant topoisomerase I inhibitors.

and phenanthridines.[3,35] Two indolocarbazoles, edotecarin[36] and BMS-250749,[3] have entered clinical trial, and two indenoisoquinolines derivatives (NSC 725776 and 724998) are under review for clinical trials (see Figure 1).[3] They have shown favorable characteristics for the development of novel anticancer agents.

Moreover, the discovery of novel TopoI inhibitors is facilitated by the improvement of a variety of biochemical and cellular assays and X-ray crystal structures. The X-ray crystal structures of human apo-TopoI[37] and TopoI−DNA complex bound with camptothecin (PDB code 1T8I),[38] topotecan (PDB code 1K4T),[39] indolocarbazole (PDB code 1SCU),[38] indenoisoquinoline (PDB code 1SC7),[38] and norindenoisoquinoline (PDB code 1TL8)[40] have been reported. The understanding of TopoI's molecular structure and mechanism of action provides insights into the physiological functions of TopoI and also provides a strong structural basis for the rational design of highly potent non-CPT TopoI inhibitors.

Structure-based virtual screening (SBVS) is becoming a powerful tool for hit identification.[41−43] In this work, we describe the rapid and successful identification of novel TopoI inhibitors using SBVS. Five hits were identified to possess both TopoI inhibitory activity and in vitro antitumor activity. After preliminary optimization of hit **20**, both antitumor activity and antitumor spectrum were improved. To the best of our knowledge, this is the first example of the successful application of SBVS to identify novel TopoI inhibitors.

Results and Discussion

Virtual Screening. The evaluation of the reliability of various docking methods for the docking of TopoI inhibitors was performed (see Supporting Information for detailed results). Gold with GoldScore fitness function was found to be the best method for TopoI−DNA−CPT complex (PDB code 1T8I). A schematic summary of the overall virtual screening procedure in this study is presented in Figure 2. A total of 287000 compounds in SPECS database (www.specs.com) were docked and ranked

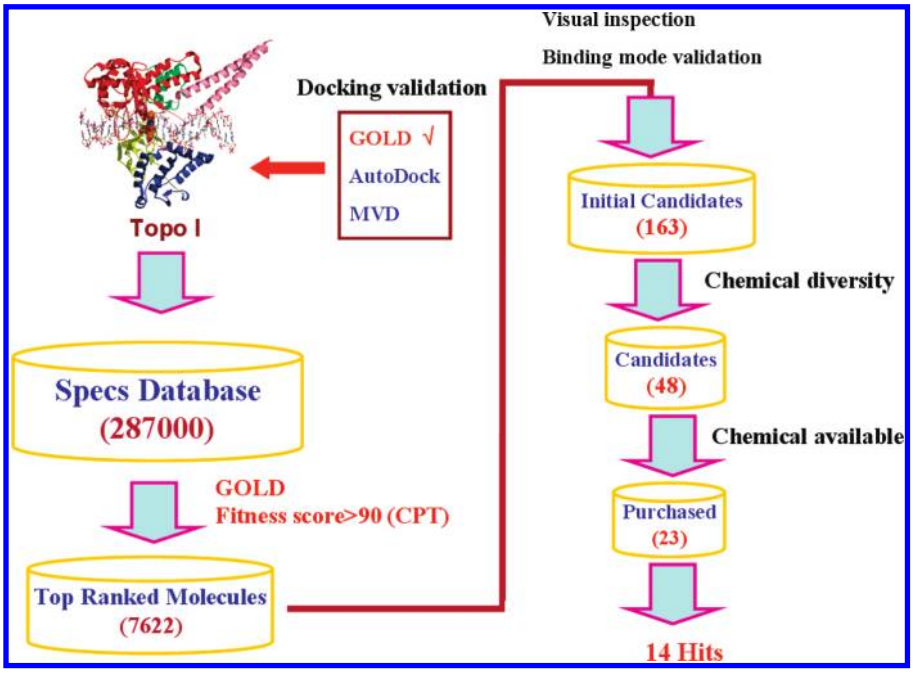

Figure 2. Flowchart of the virtual screening procedure.

with GOLD. The fitness score of CPT in the active site of TopoI (fitness score of 90) was used as a cutoff value for the selection of the initial compounds. Thus, top-ranked 7622 complexes were first selected and submitted to docking validation and visual inspection. The selection of the candidate molecules was based on the following criteria: (1) Complementarity exists between the ligand and the active site of TopoI. (2) Reasonable chemical structure and pose are in the active site of TopoI. Some unusually highly scored molecules were found to have many rotatable bonds (such as long aliphatic structures), which were excluded for further evaluation. (3) There is formation of at least one hydrogen bond between the ligand and the important residues of TopoI (such as Arg364, Asp533, and Asn722, etc). As revealed by various TopoI−inhibitor complex structures,[38,39] these residues are critical for the inhibitor binding. (4) Protonation state and the tautomeric form of the ligand have to be acceptable. (5) The binding mode of the compounds can be reproduced by at least two docking methods. As a result, 163 candidate compounds can meet the above criteria. In order to achieve good chemical diversity, the resulting 163 candidates were subsequently filtered by similarity/substructure search. For the compounds with the same scaffold, only the one with the best fitness score was kept. Consequently, 48 potential TopoI inhibitors were designated for purchase. However, only 23 compounds turned out to be commercially available for in vitro assaying (Figure 3).

In Vitro TopoI Inhibition Assay. Generally, TopoI inhibitors act by stabilizing a covalent TopoI−DNA complex called the cleavable complex. Therefore, TopoI-mediated DNA cleavage assays with purified TopoI were used to investigate the inhibitory activity of the purchased compounds with their concentrations ranging from 1 to 500 μM. The ability of compounds to stabilize the cleavable complex was evaluated by incubating TopoI and supercoiled DNA pBR322 in the presence of drugs. Cleavable complexes were revealed by the appearance of short DNA fragments when the samples were analyzed by gel electrophoresis under denaturing conditions. As shown in Figure 4, 14 of 23 compounds were discovered to be active against TopoI-mediated relaxation of supercoiled DNA at high concentrations (500 μM). The TopoI inhibition activity of 14 hits was further tested at lower concentrations with five compounds (**1**, **6**, **14**, **19**, and **21**) active at 50 μM and two compounds (**1** and **6**) active against 10 μM (see Supporting Information for details).

In Vitro Antitumor Activity. The solid tumor cell lines A-549 (for non-small-cell lung cancer), LOVO (for colon cancer), HCT116 (for colon cancer), and MDA-MB-435 (for breast cancer) were chosen for testing the in vitro antitumor activities of the compounds. CPT and irinotecan were used as the reference compounds. In order to investigate the correlation between the TopoI inhibitory activity and antitumor activity, all the purchased compounds were tested for their cytotoxicity. The results revealed that most of the compounds without TopoI inhibitory activity did not show in vitro antitumor activity. Some weak TopoI inhibitors (such as **3**, **5**, **8**, **12**, and **16**) were also inactive against the tested tumor cell lines. Among the TopoI inhibitors, five compounds (**1**, **14**, **20**, **21**, and **23**) showed moderate to good cytotoxicity. However, no in vitro antitumor activity was observed for compound **6**, the most potent TopoI inhibitor. It is well accepted that the penetration ability of cell membrane is an important factor for the cytotoxicity. Compound **6** has a carboxyl group and has difficulty crossing the cell membrane. Compounds **1** and **21**, another two potent TopoI inhibitors, also showed good in vitro antitumor activity with broad spectrum. They are active against all the three human tumor cell lines with their IC_{50} values in the range 0.50−43 μM. The potent antitumor activity of the compounds can be well related to their capacity to inhibit TopoI. Although the cytotoxicity of compounds identified from virtual screening is lower than that of CPT and irinotecan, they provide novel chemotypes for the discovery of novel antitumor agents.

Binding Mode of the New TopoI Inhibitors. In order to obtain accurate binding mode of the hits, molecular dynamics (MD) simulations were performed on the docking model of compounds **1**, **6**, **20**, and **21** (see Supporting Information for detailed computational protocols and results). We used the Desmond method (Desmond_Maestro_academic-2009-02,http://www.deshawresearch.com) to carry out all the simulations. After 2 ns of MD calculations, stable TopoI−DNA−inhibitor ternary

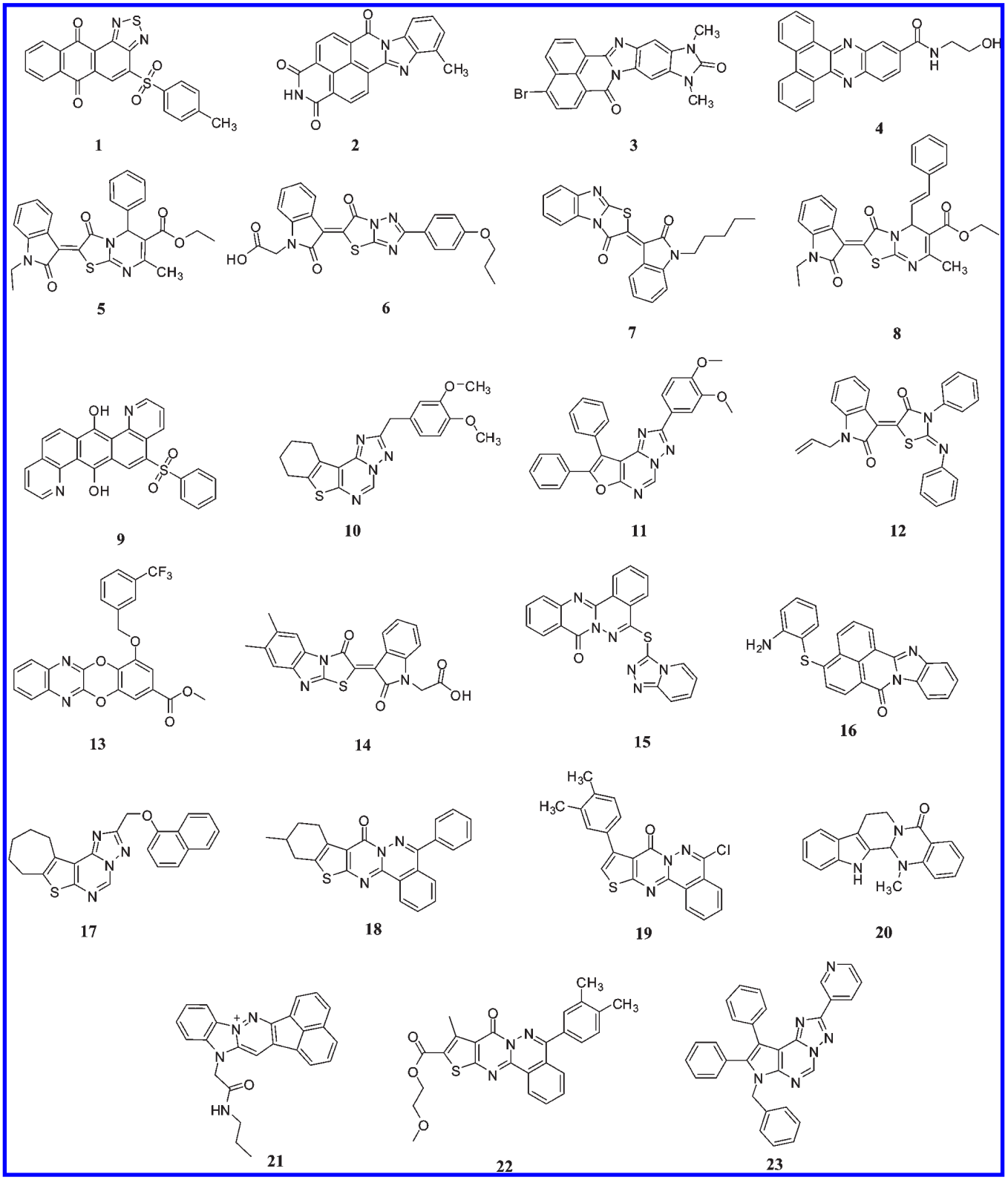

Figure 3. Chemical structures of the purchased compounds from virtual screening.

complexes were obtained. The MD results indicated that the conformation of hits in the active site of TopoI was very similar to that in the docking model (rmsd of <2 Å) and important stacking and hydrogen-bonding interactions were preserved. Although the hits represent several unique chemotypes, they were predicted to bind with the TopoI active site in a manner similar to that of the known TopoI inhibitors except compound **20** (Figure 5). Most of the compounds have planar structure, which intercalates at the site of DNA cleavage and forms base-stacking interactions with both the -1 (upstream) and $+1$ (downstream) base pairs. Moreover, they can form hydrogen-bonding interaction with the surrounding residues, such as Arg364 and Asn352. For example, compound **6** can intercalate into DNA base pairs with the thiazolotriazol ring mimicking the

BC ring of CPT and with the phenyl group mimicking the E ring of CPT (Figure 5B). The thiazolone carbonyl oxygen and triazole nitrogen can form two hydrogen bonds with Arg364. Its indol-2-one-*N*-acetic acid part is faced into the major groove, and the terminal carboxyl group forms no direct interaction with TopoI, suggesting that the carboxyl group can be replaced by a more hydrophobic group to improve its cytotoxicity. Unlike other hits, compound **20** shares "L type" conformation in the active site of TopoI (Figure 5C). Only the DE ring of **20** intercalates at the DNA cleavage site and stacks with the base pairs. Hydrogen bonding interaction is observed between its indole NH and Arg364 (Figure 5C).

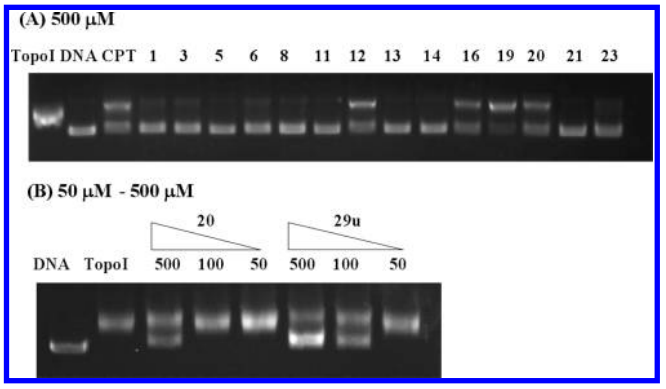

Figure 4. Gel electrophoresis of TopoI-induced DNA cleavage assay for hits from virtual screening. (A) Inhibition of TopoI relaxation activity at 500 μM: lane 1, DNA + TopoI; lane 2, supercoiled plasmid DNA; lane 3, DNA + TopoI + CPT; lanes 4−17, DNA + TopoI + hit (**1**, **3**, **5**, **6**, **8**, **11**, **12**, **13**, **14**, **16**, **19**, **20**, **21**, and **23**, respectively). (B) Inhibition of TopoI relaxation activity ranging from 50 to 500 μM: lane 1, supercoiled plasmid DNA; lane 2, DNA + TopoI; lanes 3−5, DNA + TopoI + compound **20** (500, 100, and 50 μM); lanes 6−8, DNA + TopoI + 1 (500, 100, and 50 μM).

Among the identified hits, compounds **1** and **21** showed potent activity in both TopoI inhibition assay and antitumor activity assay. The binding mode of compound **1** in the active site of TopoI is similar to that of CPT. Its orientation in the active site cavity is perpendicular to the main axis of the DNA and parallel to the bases. The planar nature of the anthrathiadiazole ring system allows it to stack with the base pairs. Hydrogen-bonding interaction was observed between the nitrogen atom of thiadiazole ring and Arg364 (Figure 5A). The 4-tosyl group was faced into the major groove and formed hydrophobic interaction with the surrounding hydrophobic residues such as Ala351 and Met428. Compound **21** is the only charged inhibitor depicted in Figure 3. Like CPT, the six-member planar ring of **21** intercalates at the site of DNA cleavage, between the +1 and −1 base pairs (Figure 5D). Its C ring is on the minor groove side of the intercalation binding pocket, and its nitrogen atom forms a hydrogen bond with Arg364 at a distance of 2.36 Å. The amide side chain of the B-ring nitrogen projects in the major groove with its amide NH forming hydrogen bonding interaction with Asn352. In summary, compounds **1**, **6**, and **21** have three common structural features: (1) a planar aromatic ring that intercalates at DNA cleavage site; (2) a heterocyclic nitrogen atom as a hydrogen bond acceptor that forms a hydrogen bond with Arg364; (3) a hydrophobic side chain that faces into the major groove. These structural features are well consistent with the known TopoI inhibitors, such as CPTs, indolocarbazoles, and indenoisoquinolines.[38]

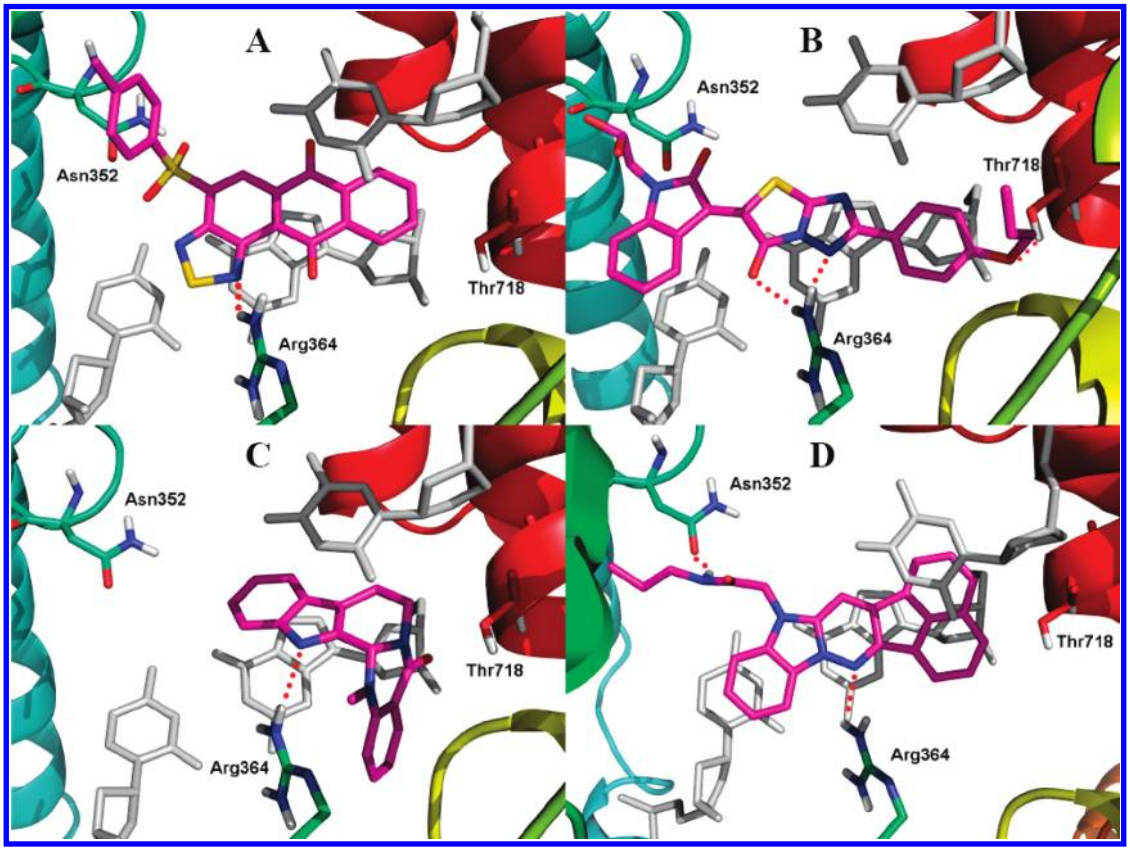

Figure 5. Schematic representation of the proposed binding mode for compounds **1** (A), **6** (B), **20** (C), and **21** (D) in the TopoI−DNA complex. The figure was generated using PyMol (http://pymol.sourceforge.net/).

Preliminary Optimization of Hit 20 and Structure−Activity Relationships. Compounds **1**, **14**, **20**, **21**, and **23** showed both TopoI inhibitory activities and potent in vitro antitumor activity (Table 1). They provided good starting points for further optimization. In the present study, compound **20** (evodiamine), a quinolone alkaloid isolated from the fruit of *Evodia rutaecarpa*,[49] was first chosen for preliminary structure−activity relationship studies. Evodiamine has shown various biological activities, including catecholamine secretion,[50] testosterone secretion,[51] antiobesity,[52] anti-inflammatory,[53] antiapoptosis,[54,55] antinociceptive,[56] vasodilatory,[57] and thermoregulatory[58] effects. However, the SAR study of evodiamine has not been reported. We chose evodiamine for hit optimization because it possesses several advantages for structural modification. (1) It is the only compound with a free N−H function from which derivatives can be readily obtained. (2) It has relatively low molecular weight (MW = 303) and is suitable for further optimization. (3) It shows the best cytotoxicity against the breast cancer cell line MDA-MB-435 (IC_{50} = 29 μM). (3) Unlike other planar hits, it binds to TopoI with "L type" conformation, which is uncommon for TopoI inhibitors.

Table 1. In Vitro Antitumor Activity of the Compounds Obtained from Virtual Screening (IC_{50}, μM)

	IC_{50}, μM		
compd	A549	LOVO	MDA-MB-435
1	0.50 ± 0.021	43 ± 1.1	25 ± 0.97
2	na[a]	na[a]	na[a]
3	na[a]	na[a]	na[a]
4	na[a]	na[a]	na[a]
5	na[a]	na[a]	na[a]
6	na[a]	na[a]	na[a]
7	na[a]	na[a]	na[a]
8	na[a]	na[a]	na[a]
9	120 ± 2.3	na[a]	na[a]
11	na[a]	75 ± 1.8	na[a]
12	na[a]	na[a]	na[a]
13	na[a]	na[a]	na[a]
14	na[a]	240 ± 29	170 ± 15
15	na[a]	na[a]	na[a]
16	na[a]	na[a]	na[a]
17	na[a]	na[a]	na[a]
18	na[a]	na[a]	na[a]
19	na[a]	190 ± 8.2	na[a]
20	na[a]	na[a]	29 ± 3.4
21	37 ± 1.6	26 ± 2.0	77 ± 7.8
22	na[a]	45 ± 3.5	na[a]
23	na[a]	180 ± 7.2	na[a]
CPT	0.057 ± 0.0018	3.1 ± 0.71	0.71 ± 0.014
IRT	6.4 ± 0.35	8.8 ± 0.31	17 ± 0.80

[a] na = not active.

From the chemical point of view, the indole NH of evodiamine is a good functional group for the synthesis of various derivatives. The docking model also revealed that evodiamine only partly intercalated into the DNA base pairs (DE ring) and the attachment of an aromatic group to the indole NH could improve the base-stacking interactions with TopoI. In order to keep the hydrogen bonding interaction with Arg364, a proper linker between the aromatic group and the indole NH is needed to interact with Arg364. As a result, *N*-benzoylevodiamine derivatives were selected from molecular docking studies. Figure 6 illustrated the binding mode of compound **29u**. The position of 4-chlorine benzoyl group of compound **29u** in the active site of TopoI was similar to the position of the BC ring of CPT and formed additional base-stacking interactions with both the −1 (upstream) and +1 (downstream) base pairs (Figure 6B). Especially, its carbonyl oxygen atom could also form hydrogen bonding interaction with Arg364. Therefore, a series of *N*-benzoylevodiamine analogues were designed and synthesized. In order to investigate the structure−activity relationship (SAR), *N*-alkyl, benzyl, cyano, and ester evodiamine derivatives were also prepared.

The synthetic route of compounds **29a**−**x** is depicted in Scheme 1. Evodiamine was synthesized by the reported procedure (Scheme 1).[44−48] Starting from **24**, it was converted to amide **25** by reacting with ethyl formate. In the presence of $POCl_3$, the key intermediate ABC ring **26** was obtained by ring closure reaction of amide **25**. On the other hand, reacting 2-(methylamino)benzoic acid **27** with ClCOOEt afforded isatoic anhydride **28**. Evodiamine was obtained by ring closure reaction

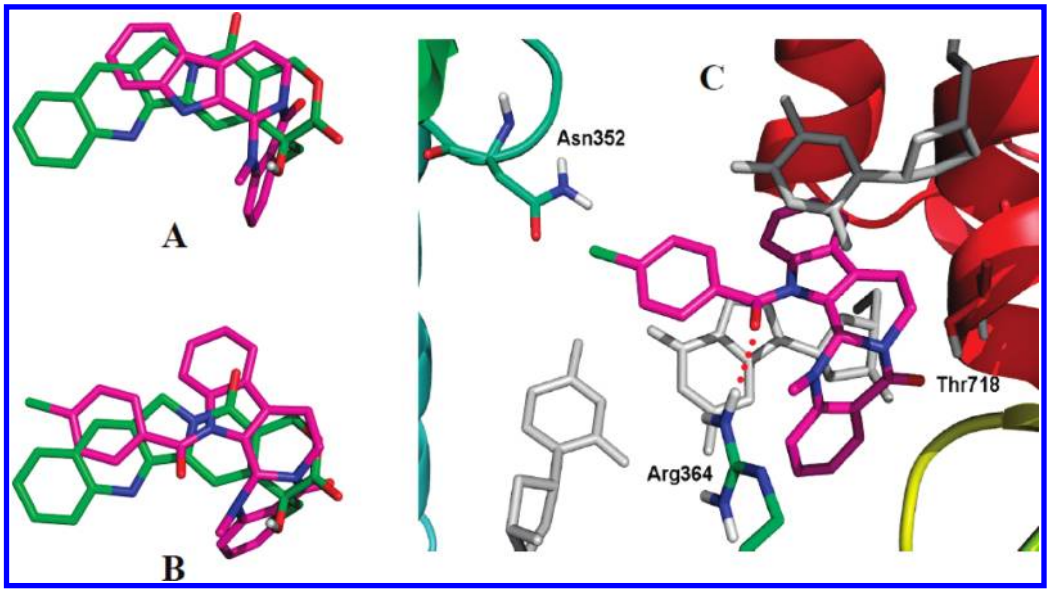

Figure 6. (A) Superimposition of the docked conformations of **20** with CPT. (B) Superimposition of the docked conformations of **29u** with CPT. (C) Binding mode of compounds **29u** in the active site of TopoI−DNA complex. The figure was generated using PyMol (http://pymol.sourceforge.net/).

Scheme 1[a]

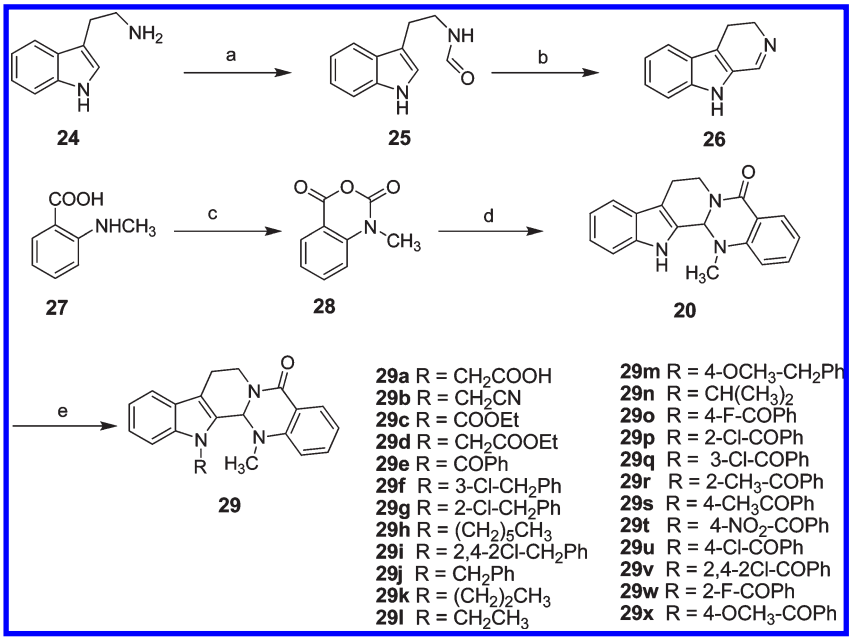

[a] Reagents and conditions: (a) HCOOEt, reflux, 12 h, yield 84%; (b) $POCl_3$, CH_2Cl_2, 0 2 h, room temp 2 h, yield 55%; (c) ClCOOEt, reflux, 12 h, yield 60%; (d) **26**, CH_2Cl_2, 30−60 °C, 6 h, yield 70%; (e) RX, NaH, DMF, 80 °C, 24 h, yield 11−79%.

Table 2. In Vitro Antitumor Activity of the N-Substituted Evodiamine Analogues (IC_{50}, μM)

	IC_{50}, μM		
compd	A549	LOVO	MDA-MB-435
29a	72 ± 2.3	130 ± 10	13 ± 0.81
29b	220 ± 7.9	na[a]	200 ± 4.6
29c	130 ± 3.7	95 ± 7.3	9.4 ± 0.54
29d	na[a]	na[a]	150 ± 7.6
29e	10 ± 0.60	15 ± 0.39	0.047 ± 0.0015
29f	na[a]	na[a]	na[a]
29g	29 ± 1.3	74 ± 1.6	42 ± 0.50
29h	120 ± 4.2	59 ± 6.9	110 ± 5.3
29i	na[a]	na[a]	na[a]
29j	55 ± 2.4	67 ± 3.3	110 ± 3.7
29k	na[a]	na[a]	na[a]
29l	na[a]	na[a]	na[a]
29m	na[a]	na[a]	na[a]
29n	na[a]	na[a]	na[a]
CPT	0.057 ± 0.0030	3.1 ± 0.067	0.71 ± 0.031
IRT	6.4 ± 0.27	8.8 ± 0.10	17 ± 0.95

[a] na = not active.

between **28** and carboline **26**. In the presence of NaH and DMF, evodiamine was treated with various RX reagents (such as substituted benzolyl chloride, substituted benzyl chloride, alkyl chloride, etc.) to afford the compounds **29a**−**x**.

In vitro TopoI inhibition assay indicated that the *N*-benzoyl analogue **29u** showed higher activity than evodiamine. Compound **29u** was active against TopoI-mediated relaxation of supercoiled DNA at 100 μM, which is consistent with the docking model of evodiamine and **29u**. Moreover, improved in vitro antitumor activities and spectrum of evodiamine derivatives were also observed (Tables 2 and 3). Evodiamine is only active against the breast cancer cell line. After the introduction of an ethyl carboxylate group on the indole NH (compound **29c**), both cytotoxicity and antitumor spectrum were improved. The IC_{50} values of compound **29c** are in the range 9.4−130 μM. The insertion of a methylene group between indole NH and carboxylate group of compound **29c** resulted in a decrease of the

Table 3. In Vitro Antitumor Activity of the N-Substituted Benzoxyl Evodiamine Analogues (IC_{50}, μM)

	IC_{50}, μM		
compd	A549	MDA-MB-435	HCT116
29o	4.3 ± 0.21	0.13 ± 0.011	5.1 ± 0.27
29p	14 ± 3.1	0.18 ± 0.014	4.7 ± 0.066
29q	2.9 ± 0.082	0.051 ± 0.0029	3.3 ± 0.12
29r	4.2 ± 0.33	0.15 ± 0.0063	3.9 ± 0.041
29s	3.0 ± 0.17	0.038 ± 0.0032	4.3 ± 0.022
29t	2.8 ± 0.031	0.55 ± 0.026	4.1 ± 0.19
29u	0.86 ± 0.044	0.049 ± 0.0030	2.6 ± 0.083
29v	5.3 ± 0.38	0.39 ± 0.034	3.8 ± 0.066
29w	35 ± 0.46	na[a]	89 ± 0.93
29x	74 ± 9.1	na[a]	45 ± 4.0

[a] na = not active.

activity. Compound **29d** lost activity against lung cancer and colon cancer cell lines again. When compound **29d** was hydrolyzed to compound **29a**, the cytotoxicity and spectrum were improved again. Compound **29e**, bearing a benzoyl substituent, showed good inhibitory effects against all the three cancer cell lines with IC_{50} values in the range 0.047−15 μM. Remarkably, compound **29e** was particularly effective against breast cancer cell line, which was more potent than the reference drugs CPT and irinotecan. The replacement of the benzoyl group of compound **29e** by a benzyl group (compound **29j**) resulted in a decrease of the cytotoxicity to a large extent. For compound **29j**, the addition of a chlorine at position 2 of the benzyl group (compound **29g**) led to a slight increase of the cytotoxicity. On the other hand, a loss of the cytotoxicity was observed for 3-Cl (compound **29f**), 2,4-dichloro (compound **29i**), and 4-methoxyl (compound **29m**) derivatives. Furthermore, most of the alkyl derivatives (e.g., **29k**, **29l**, and **29n**) proved to be totally inactive. Only compound **29h** showed moderate activity.

Because *N*-benzoyl derivative (compound **29e**) revealed good cytotoxicity with broad spectrum, we further introduced various substituents on the benzoyl group (compounds **29o**−**x**). It can be seen that the cytotoxic potency of the compounds varies

considerably depending on the type and position of the substituents. Compared with compound **29e**, several compounds (e.g., **29s** and **29u**) showed improved activity. In general, 4-substituted derivatives were more potent than 2-substituted and 3-substituted derivatives. For example, compound **29u** showed higher cytotoxicity than compounds **29p** and **29q**. For the 4-substituted derivatives, halogens (i.e., chlorine and fluorine) and methyl group are favorable for the cytotoxicity. In comparison with the monochlorine substituted compounds (compounds **29p** and **29u**), the disubstituted derivative (compound **29v**) led to a decrease of the cytotoxicity. Remarkably, the IC_{50} values of compound **29u** against A549, MDA-MB435, and HCT116 cell lines are 0.86, 0.049, and 2.6 μM, respectively, suggesting that it is a promising lead for the discovery of novel anticancer agents.

Conclusion

From the above results, we can find that molecular weight and synthetic possibility should be considered as two important factors for the selection of hits for structural optimization. In most cases, the molecular weight and hydrophobicity will be increased during the process of hit-to-lead and lead-to-candidate. A starting structure with relatively low molecular weight is more likely to be optimized to druglike candidates. On the other hand, the synthetic possibility is also a major problem for natural product-like hits from virtual screening. Evodiamine has a free amine group with moderate molecular weight, which can be easily transformed to active derivatives with druglike properties. This example might give us some useful information about hit selection after SBVS studies. Such structural requirement, a scaffold with a free N−H group and molecular weight of about 350, could be included in the next SBVS study.

Evodiamine shares an interesting "L type" conformation in the active site of topo1−DNA cleavable complex. Its free indole N−H function is a good site for chemical derivatization. However, the hydrogen bond with Arg364 would be broken if the indole amine was substituted. In order to address the contradiction, proper functional group transformation to keep the hydrogen bonding interaction is an efficient method to retain the binding affinity. In the present study, the indole amine was transferred to the amide and its carbonyl group can also form a hydrogen bond with Arg364. By means of this method, we think a key N−H group participating in a special binding mode is amenable to further chemistry and can be transformed to generate active derivatives.

Experimental Section

Chemistry. General Methods. ^{1}H NMR and ^{13}C NMR spectra were recorded on a Bruker Avance 300 spectrometer (Bruker Company, Germany), using TMS as an internal standard and $CDCl_3$ or DMSO-d_6 as solvent. Chemical shifts are given in ppm (δ). Elemental analyses were performed with a MOD-1106 instrument and were consistent with theoretical values within 0.4%. The mass spectra were recorded on an Esquire 3000 LC−MS mass spectrometer. Silica gel thin-layer chromatography was performed on precoated plates GF-254 (Qingdao Haiyang Chemical, China). The purity of final compounds was assessed on the basis of analytical HPLC, and the results were greater than 95%. All solvents and reagents were analytically pure, and no further purification was needed. All starting materials were commercially available.

General Procedure for the Synthesis of Compounds 29a−x. NaH (60% oil, 6.6 mmol) was suspended in a solution of evodiamine[44−48] (0.20 g, 0.66 mmol) in DMF (20 mL). The reacting mixture was heated to 80 °C and stirred for 24 h. The mixture was diluted with H_2O (50 mL) and then extracted with EtOAc (50 mL × 3). The extract was washed with saturated NaCl solution (50 mL × 3), dried over anhydrous Na_2SO_4, and concentrated under reduced pressure. The residue was purified by column chromatography (EtOAc/hexane = 1:4) to give compounds **20a−x** with moderate to good yields.

***N*-Acetic Acid Evodiamine (29a).** Yield 60%, yellow oil. ^{1}H NMR (DMSO, 500 MHz) δ 2.41 (s, 3H), 2.85 (m, 1H), 3.05 (m, 1H), 3.17 (m, 1H), 4.80 (m, 1H), 5.07 (dd, 2H, J_1 = 18.1 Hz, J_2 = 18.1 Hz), 6.02 (s, 1H), 7.02−8.01 (m, 8H). ESI-MS (*m*/*z*): 362.2 [M + 1]. Anal. ($C_{21}H_{19}N_3O_3$) C, H, N.

***N*-Acetonitrile Evodiamine (29b).** Yield 44%, white solid. ^{1}H NMR (DMSO, 500 MHz) δ 2.39 (s, 3H), 2.82 (m, 1H), 2.98 (m, 1H), 3.14 (m, 1H), 4.66 (m, 1H), 5.57 (s, 2H), 6.21 (s, 1H), 7.21−7.95 (m, 8H). ^{13}C NMR ($CDCl_3$, 500 MHz) δ 20.08, 31.73, 36.97, 39.00, 67.89, 109.02, 114.44, 115.51, 119.54, 121.22, 123.61, 124.00, 124.24, 125.04, 126.32, 127.60, 129.00, 133.14, 136.92, 150.47, 164.34. ESI-MS (*m*/*z*): 343.74 [M + 1]. Anal. ($C_{21}H_{18}N_4O$) C, H, N.

***N*-Ethyl Formate Evodiamine (29c).** Yield 11%, yellow solid. ^{1}H NMR ($CDCl_3$, 500 MHz) δ 1.29 (t, 3H, J = 6.7 Hz), 2.45 (s, 3H), 2.86 (m, 1H), 2.99 (m, 1H), 3.20 (m, 1H), 4.45 (m, 2H), 4.91 (m, 1H), 6.29 (s, 1H), 7.04−8.27 (m, 8H). ESI-MS (*m*/*z*): 376.45 [M + 1]. Anal. ($C_{22}H_{21}N_3O_3$) C, H, N.

***N*-Ethyl Acetate Evodiamine (29d).** Yield 44%, yellow solid. ^{1}H NMR ($CDCl_3$, 500 MHz) δ 1.25 (t, 3H), 2.40 (s, 3H), 2.84 (m, 1H), 3.03 (m, 1H), 3.24 (m, 1H), 4.20 (m, 2H), 4.92 (m, 1H), 4.93 (d, 1H), 5.15 (d, 1H), 5.93 (s, 1H), 7.15−8.23 (m, 8H). ^{13}C NMR ($CDCl_3$, 500 MHz) δ 14.13, 20.16, 36.66, 39.20, 45.21, 60.47, 68.00, 109.09, 113.89, 119.08, 120.17, 123.10, 123.33, 124.28, 124.52, 125.92, 128.40, 128.93, 132.84, 137.77, 150.83, 164.42, 168.54. ESI-MS (*m*/*z*): 390.35 [M + 1]. Anal. ($C_{23}H_{23}N_3O_3$) C, H, N.

***N*-Benzoylevodiamine (29e).** Yield 37%, yellow solid. ^{1}H NMR ($CDCl_3$, 500 MHz) δ 2.43 (s, 3H), 2.92 (m, 1H), 3.05 (m, 1H), 3.18 (m, 1H), 4.90 (m, 1H), 5.94 (s, 1H), 7.15−8.15 (m, 13H). ESI-MS (*m*/*z*): 408.84 [M + 1]. Anal. ($C_{26}H_{21}N_3O_2$) C, H, N.

***N*-(3-Chlorobenzyl)evodiamine (29f).** Yield 67%, yellow solid. ^{1}H NMR ($CDCl_3$, 500 MHz) δ 2.35 (s, 3H), 2.95 (m, 1H), 3.06 (m, 1H), 3.21 (m, 1H), 4.90 (m, 1H), 5.38 (d, 1H, J = 16.8 Hz), 5.65 (d, 1H, J = 16.8 Hz), 5.81 (s, 1H), 6.88−8.11 (m, 12H). ESI-MS (*m*/*z*): 428.61 [M + 1]. Anal. ($C_{26}H_{22}ClN_3O$) C, H, N.

***N*-(2-Chlorobenzyl)evodiamine (29g).** Yield 75%, yellow solid. ^{1}H NMR ($CDCl_3$, 500 MHz) δ 2.40 (s, 3H), 2.96 (m, 1H), 3.07 (m, 1H), 3.21 (m, 1H), 4.91 (m, 1H), 5.54 (d, 1H, J = 17.7 Hz), 5.78 (d, 1H, J = 17.8 Hz), 6.36 (s, 1H), 6.99−8.08 (m, 12H). ESI-MS (*m*/*z*): 428.90 [M + 1]. Anal. ($C_{26}H_{22}ClN_3O$) C, H, N.

***N*-Hexylevodiamine (29h).** Yield 27%, yellow solid. ^{1}H NMR ($CDCl_3$, 500 MHz) δ 0.84 (t, 3H), 1.25−1.83 (m, 8H), 2.40 (s, 3H), 2.93 (m, 1H), 3.02 (m, 1H), 3.19 (m, 1H), 4.17 (t, 2H, J = 7.5 Hz), 4.90 (m, 1H), 5.96 (s, 1H), 7.15−8.15 (m, 8H). ESI-MS (*m*/*z*): 488.93 [M + 1]. Anal. ($C_{25}H_{29}N_3O$) C, H, N.

***N*-(2,4-Dichlorobenzyl)evodiamine (29i).** Yield 36%, yellow solid. ^{1}H NMR ($CDCl_3$, 500 MHz) δ 2.39 (s, 3H), 2.95 (m, 1H), 3.07 (m, 1H), 3.21 (m, 1H), 4.92 (m, 1H), 5.46 (d, 1H, J = 16.7 Hz), 5.76 (d, 1H, J = 16.7 Hz), 6.31 (s, 1H), 6.97−8.09 (m, 11H). ESI-MS (*m*/*z*): 462.68 [M]. Anal. ($C_{26}H_{21}Cl_2N_3O$) C, H, N.

***N*-Benzylevodiamine (29j).** Yield 58%, yellow solid. ^{1}H NMR ($CDCl_3$, 500 MHz) δ 2.38 (s, 3H), 2.93 (m, 1H), 3.06 (m, 1H), 3.19 (m, 1H), 4.91 (m, 1H), 5.44 (d, 1H, J = 16.7 Hz), 5.68 (d, 1H, J = 16.7 Hz), 5.81 (s, 1H), 7.00−8.10 (m, 13H). ESI-MS (*m*/*z*): 394.72 [M + 1]. Anal. ($C_{26}H_{23}N_3O$) C, H, N.

***N*-Propylevodiamine (29k).** Yield 79%, yellow solid. ^{1}H NMR ($CDCl_3$, 500 MHz) δ 0.95 (t, 3H, J = 7.4 Hz), 1.86 (m, 2H), 2.40 (s, 3H), 2.89 (m, 1H), 3.02 (m, 1H), 3.19 (m, 1H), 4.17 (m, 1H), 4.31 (m, 1H), 4.92 (m, 1H), 5.97 (s, 1H), 7.17−8.15 (m, 8H). ESI-MS (*m*/*z*): 346.68 [M + 1]. Anal. ($C_{22}H_{23}N_3O$) C, H, N.

***N*-Ethylevodiamine (29l).** Yield 64%, yellow solid. ^{1}H NMR ($CDCl_3$, 500 MHz) δ 1.42 (t, 3H, J = 7.2 Hz), 2.42 (s, 3H), 2.89 (m, 1H), 3.02 (m, 1H), 3.19 (m, 1H), 4.24 (m, 1H), 4.43 (m, 1H), 4.92 (m, 1H), 5.97 (s, 1H), 7.17−8.15 (m, 8H). ^{13}C NMR ($CDCl_3$, 500 MHz) δ 15.16, 20.21, 29.52, 36.25, 39.16, 67.78,

109.44, 109.45, 112.76, 118.85, 119.35, 122.40, 122.93, 123.97, 125.63, 127.92, 128.77, 132.67, 136.63, 150.77, 164.36. ESI-MS (m/z): 332.83 [M + 1]. Anal. ($C_{21}H_{21}N_3O$) C, H, N.

***N*-(4-Methoxylbenzyl)evodiamine (29m).** Yield 36%, yellow solid. ^{1}H NMR ($CDCl_3$, 500 MHz) δ 2.39 (s, 3H), 2.92 (m, 1H), 3.03 (m, 1H), 3.14 (m, 1H), 3.73 (s, 3H), 4.88 (m, 1H), 5.38 (d, 1H, J = 16.7 Hz), 5.68 (d, 1H, J = 16.7 Hz), 5.81 (s, 1H), 6.74−7.62 (m, 12H). ESI-MS (m/z): 424.65 [M + 1]. Anal. ($C_{27}H_{25}N_3O_2$) C, H, N.

***N*-Isopropylevodiamine (29n).** Yield 66%, yellow solid. ^{1}H NMR (DMSO, 300 MHz) δ 1.49 (d, 3H, J = 6.9 Hz), 1.70 (d, 3H, J = 6.9 Hz), 2.37 (s, 3H), 2.95 (m, 1H), 3.03 (m, 1H), 3.17 (m, 1H), 4.66 (m, 1H), 4.82 (m, 1H), 6.13 (s, 1H), 7.04−7.94 (m, 8H). ESI-MS (m/z): 346.37 [M + 1]. Anal. ($C_{22}H_{23}N_3O$) C, H, N.

***N*-(4-Fluorobenzoyl)evodiamine (29o).** Yield 32%, yellow solid. ^{1}H NMR (DMSO, 300 MHz) δ 2.45 (s, 3H), 2.86 (m, 1H), 3.02 (m, 1H), 3.22 (m, 1H), 4.67 (m, 1H), 5.89 (s, 1H), 7.01−8.02 (m, 12H). ESI-MS (m/z): 448.31 [M + Na]. Anal. ($C_{26}H_{20}FN_3O_2$) C, H, N.

***N*-(2-Chlorobenzoyl)evodiamine (29p).** Yield 52%, yellow solid. ^{1}H NMR ($CDCl_3$, 500 MHz) δ 2.41 (s, 3H), 2.90 (m, 1H), 3.04 (m, 1H), 3.21 (m, 1H), 4.78 (m, 1H), 5.74 (s, 1H), 6.98−8.01 (m, 12H). ^{13}C NMR ($CDCl_3$, 500 MHz) δ 20.44, 36.00, 37.64, 67.84, 115.37, 118.92, 121.92, 122.86, 123.31, 123.60, 123.93, 126.19, 126.41, 127.61, 127.97, 128.55, 129.82, 130.91, 131.73, 131.88, 132.51, 132.84, 133.81, 134.60, 150.14, 164.41. ESI-MS (m/z): 464.83 [M + Na]. Anal. ($C_{26}H_{20}ClN_3O_2$) C, H, N.

***N*-(3-Chlorobenzoyl)evodiamine (29q).** Yield 58%, yellow solid. ^{1}H NMR (DMSO, 300 MHz) δ 2.40 (s, 3H), 2.88 (m, 1H), 3.03 (m, 1H), 3.20 (m, 1H), 4.65 (m, 1H), 5.76 (s, 1H), 7.01−8.02 (m, 12H). ESI-MS (m/z): 465.03 [M + Na]. Anal. ($C_{26}H_{20}ClN_3O_2$) C, H, N.

***N*-(2-Methylbenzoyl)evodiamine (29r).** Yield 58%, yellow solid. ^{1}H NMR (DMSO, 300 MHz) δ 2.26 (s, 3H), 2.40 (s, 3H), 2.91 (m, 1H), 3.05 (m, 1H), 3.14 (m, 1H), 4.64 (m, 1H), 5.75 (s, 1H), 7.01−8.02 (m, 12H). ESI-MS (m/z): 445.36 [M + Na]. Anal. ($C_{27}H_{23}N_3O_2$) C, H, N.

***N*-(4-Methylbenzoyl)evodiamine (29s).** Yield 54%, white solid. H NMR (DMSO, 300 MHz) δ 2.30 (s, 3H), 2.36 (s, 3H), 2.87 (m, 1H), 3.03 (m, 1H), 3.17 (m, 1H), 4.65 (m, 1H), 5.75 (s, 1H), 6.99−7.82 (m, 12H). ^{13}C NMR ($CDCl_3$, 500 MHz) δ 20.55, 21.62, 36.48, 38.01, 68.08, 114.41, 119.03, 121.14, 122.79, 123.45, 123.82, 124.97, 127.33, 128.57, 128.91, 128.98, 129.30, 129.53, 129.76, 130.02, 132.06, 132.82, 137.70, 143.93, 150.61, 164.53, 168.69. ESI-MS (m/z): 445.09 [M + Na]. Anal. ($C_{27}H_{23}N_3O_2$) C, H, N.

***N*-(4-Nitrobenzoyl)evodiamine (29t).** Yield 44%, yellow solid. ^{1}H NMR (DMSO, 300 MHz) δ 2.21 (s, 3H), 2.89 (m, 1H), 3.00 (m, 1H), 3.15 (m, 1H), 4.64 (m, 1H), 5.74 (s, 1H), 6.95−7.97 (m, 12H). ESI-MS (m/z): 453.63 [M + 1]. Anal. ($C_{26}H_{20}N_4O_4$) C, H, N.

***N*-(4-Chlorobenzoyl)evodiamine (29u).** Yield 57%, yellow solid. ^{1}H NMR (DMSO, 300 MHz) δ 2.32 (s, 3H), 2.89 (m, 1H), 3.02 (m, 1H), 3.21 (m, 1H), 4.64 (m, 1H), 5.75 (s, 1H), 6.92−8.03 (m, 12H). ESI-MS (m/z): 465.19 [M + Na]. Anal. ($C_{26}H_{20}ClN_3O_2$) C, H, N.

***N*-(2,4-Dichlorobenzoyl)evodiamine (29v).** Yield 61%, yellow solid. ^{1}H NMR ($CDCl_3$, 500 MHz) δ 2.33 (s, 3H), 2.89 (m, 1H), 3.03 (m, 1H), 3.15 (m, 1H), 4.92 (m, 1H), 5.83 (s, 1H), 7.03−8.03 (m, 11H). ESI-MS (m/z): 477.02 [M + 1]. Anal. ($C_{26}H_{19}Cl_2N_3O_2$) C, H, N.

***N*-(2-Fluorobenzoyl)evodiamine (29w).** Yield 54%, yellow solid. ^{1}H NMR ($CDCl_3$, 300 MHz) δ 2.32 (s, 3H), 2.95 (m, 1H), 3.02 (m, 1H), 3.16 (m, 1H), 4.90 (m, 1H), 5.35 (s, 1H), 7.06−8.04 (m, 12H). ESI-MS (m/z): 424.98 [M]. Anal. ($C_{26}H_{20}FN_3O_2$) C, H, N.

***N*-(4-Methoxybenzoyl)evodiamine (29x).** Yield 59%, yellow solid. ^{1}H NMR (DMSO, 300 MHz) δ 2.32 (s, 3H), 2.86 (m, 1H), 3.02 (m, 1H), 3.17 (m, 1H), 3.82 (s, 3H), 4.66 (m, 1H), 5.86 (s, 1H), 6.98−7.75 (m, 12H). ^{13}C NMR ($CDCl_3$, 500 MHz) δ 20.45, 36.49, 37.98, 55.37, 68.00, 113.89, 113.91, 114.13, 118.96, 120.69, 122.39, 122.51, 123.40, 123.68, 124.71, 126.79, 127.19, 128.47, 129.61, 132.00, 132.70, 137.64, 150.57, 163.51, 164.37, 167.93. ESI-MS (m/z): 448.93 [M + 1]. Anal. ($C_{27}H_{23}N_3O_3$) C, H, N.

Computational Protocols. Protein Preparation. The crystallographic coordinates of the ternary complex of CPT−DNA−TopoI (3.0 Å resolution, R_{cryst} = 0.244) were obtained from the Brookhaven Protein Databank entry 1T8I.[38] All crystallographic water molecules were removed from the coordinate set. The binding region was defined as all the atoms that are 15 Å around the centroid of CPT in the crystal structure.

Validation of the Docking Methods. The ligands were extracted from the X-ray complexes, which were subsequently docked into their corresponding proteins by means of Gold 3.0.1,[59] MolDock(MVD),[60] Autodock 3.0,[61] and Autodock 4.0[61,62] software. The docking results were evaluated through a comparison between the resulting docked positions of the ligand and the experimental ones. As a measure of docking reliability, the rmsd value between the positions of heavy atoms of the ligand in the calculated and experimental structures was taken into account.

Gold 3.0.1. Docking runs were performed using the program GOLD 3.0.1, and the standard default settings were used in all calculations. For each of the 10 independent genetic algorithm runs, a default maximum of 10 000 genetic operations was performed, using the default operator weights and a population size of 100 chromosomes. Two docking analyses were carried out. In the first case, GoldScore was used. Default cutoff values of 2.5 Å for hydrogen bonds and 4.0 Å for van der Waals interactions were employed. In the second one, ChemScore was used with the default setting. Early termination was allowed if the top three solutions were within rmsd value of 1.5 Å. The docking pose analysis was carried out for the pose that got the highest score.

MolDock (MVD). MVD recognized DNA as ligand of TopoI. So we converted it to cofactor before docking. The cavity reference ligand was used for docking calculations using MolDock SE as searcher algorithm. During docking the binding site radius was set to 10 Å. Other parameters were default. In addition to MolDock Score, MolDock Score [grid] was also calculated for each compound. All of the two fitness functions used the default setting. The best docking conformations were selected on the basis of docking energies.

Autodock 3.0 and 4.0. Autodock Tools was used to check and prepare the ligands and receptors files. A grid of 44, 44, and 42 points in the x, y, and z directions was constructed centered on the center of the mass of the inhibitors. We used a grid spacing of 0.375 Å and a distance-dependent function of the dielectric constant for the energetic map calculations. Lamarckian genetic algorithm was used. The docked compounds were subjected to 50 runs of the Autodock search, using 500 000 steps of energy evaluation and the default values of the other parameters. Cluster analysis was performed on the results using an rms tolerance of 1.0 Å. The docking pose analysis was carried out for the first pose of the first cluster and the first pose of the most populated cluster.

Virtual Screening. The GOLD program (version 3.0.1) was applied to screen the SPECS database consisting of approximately 287000 compounds. The crystal structure of TopoI in complex with CPT (PDB code 1T8I) was used as the template for docking. Twenty genetic algorithm (GA) runs were performed for each molecule. For each GA run, 100 000 operations were applied on a set of five islands with a population size of 100. The weights for three types of operations (crossover, mutation, and migration) were chosen as 95%, 95%, and 10%, respectively. The selection pressure, which is the ratio of the probability of the most fit member selected as a parent to the probability of an average member selected as a parent, was set to 1:1. The annealing parameters of van der Waals and hydrogen bonding were set to 4.0 and 2.5 Å to allow a few bad bumps and poor hydrogen bonds at the beginning of a GA run. The "early termination" option was turned off to allow the continued docking even though the first three docking solutions were very similar, with rmsd values less than 1.5 Å. Moreover, analysis of

various TopoI−inhibitor complex structures revealed important hydrogen bonding interactions with Arg364. Therefore, hydrogen bond constraints with a constraint weight of 10 were applied to specify that Arg364 should form the H-bond with the docked compounds. Absence of the hydrogen bonding interactions with Arg364 was penalized by the value of 10 in the GoldScore function. GoldScore implemented in GOLD was applied to rank the docked compounds.

Enzyme Inhibition Assay. The enzyme activity was measured by assessing relaxation of supercoiled pBR322 plasmid DNA. Test compounds were dissolved in DMSO and were tested at final concentrations of 500, 100, 50, 10, and 1 μM. The reaction mixture contained 10× DNA TopoI buffer (2 μL), 0.1% BSA (2 μL), TopoI (0.5 U), the test compounds (various concentrations), pBR322 plasmid DNA (0.25 μg), and distilled water (varied as needed to bring the final volume to 20 μL) in a final volume of 20 μL. Reactions were carried out for 15 min at 37 °C and then stopped by adding SDS (0.5% final concentration). After that, 3.5 μL of 6× loading buffer (0.1 mM EDTA, 7% glycerol, 0.01% xylene cyanol FF, bromopenol blue 0.01%) was added. Reaction products were electrophoresed on a 0.8% agarose gel in TAE (Tris−acetate−EDTA) running buffer at 120 V for 40 min. To visualize the reaction products, the gel was stained with 0.5 μg/mL ethidium bromide for 10 min. DNA bands were visualized using a UV transilluminator.

In Vitro Cytotoxicity Assay. One-thousand-two-hundred cells per well were plated in 96-well plates. After culturing for 24 h, test compounds were added onto triplicate wells with different concentrations and 0.1% DMSO for control. After 3 days of incubation, 20 μL of MTT (3-[4,5-dimethylthiazol-2-yl]-2,5-diphenyltetrazolium bromide) solution (5 mg/mL) was added to each well, and after the samples were shaken for 1 min the plate was incubated further for 4 h. Formazan crystals were dissolved with 100 μL of DMSO. The absorbance (OD) was quantitated with microplate spectrophotometer at 570 nm. Wells containing no drugs were used as blanks for the spectrophotometer. The survival of the cells was expressed as percentage of untreated control wells.

Acknowledgment. This work was supported by National Natural Science Foundation of China (Grant No. 30930107), Shanghai Rising-Star Program (Grant No. 09QA1407000), and Shanghai Leading Academic Discipline Project (Project No. B906).

Supporting Information Available: Computational details and results of docking methods validation and molecular dynamic simulations; Tanimoto similarity indices between purchased compounds and camptothecin; results of TopoI inhibitory activity for hits at lower concentrations. This material is available free of charge via the Internet at http://pubs.acs.org.

References

(1) Pommier, Y. Topoisomerase I inhibitors: camptothecins and beyond. *Nat. Rev. Cancer* **2006**, *6*, 789–802.
(2) Tse, Y. C.; Kirkegaard, K.; Wang, J. C. Covalent bonds between protein and DNA. Formation of phosphotyrosine linkage between certain DNA topoisomerases and DNA. *J. Biol. Chem.* **1980**, *255*, 5560–5565.
(3) Pommier, Y. DNA topoisomerase I inhibitors: chemistry, biology, and interfacial inhibition. *Chem. Rev.* **2009**, *109*, 2894–2902.
(4) Hsiang, Y. H.; Hertzberg, R.; Hecht, S.; Liu, L. F. Camptothecin induces protein-linked DNA breaks via mammalian DNA topoisomerase I. *J. Biol. Chem.* **1985**, *260*, 14873–14878.
(5) Wall, M. E.; Wani, M. C.; Cook, C. E.; Palmer, K. H.; McPhail, A. T.; Sim, G. A. The isolation and structure of camptothecin, a novel alkaloidal leukemia and tumor inhibitor from *Camptotheca acuminata*. *J. Am. Chem. Soc.* **1966**, *88*, 3888–3890.
(6) D'Arpa, P.; Beardmore, C.; Liu, L. F. Involvement of nucleic acid synthesis in cell killing mechanisms of topoisomerase poisons. *Cancer Res.* **1990**, *50*, 6919–6924.
(7) Liu, L. F.; Desai, S. D.; Li, T. K.; Mao, Y.; Sun, M.; Sim, S. P. Mechanism of action of camptothecin. *Ann. N.Y. Acad. Sci.* **2000**, *922*, 1–10.
(8) Tsao, Y. P.; D'Arpa, P.; Liu, L. F. The involvement of active DNA synthesis in camptothecin-induced G2 arrest: altered regulation of p34cdc2/cyclin B. *Cancer Res.* **1992**, *52*, 1823–1829.
(9) Driver, R. W.; Yang, L. X. Synthesis and pharmacology of new camptothecin drugs. *Mini-Rev. Med. Chem.* **2005**, *5*, 425–439.
(10) Li, Q. Y.; Zu, Y. G.; Shi, R. Z.; Yao, L. P. Review camptothecin: current perspectives. *Curr. Med. Chem.* **2006**, *13*, 2021–2039.
(11) Thomas, C. J.; Rahier, N. J.; Hecht, S. M. Camptothecin: current perspectives. *Bioorg. Med. Chem.* **2004**, *12*, 1585–1604.
(12) Kingsbury, W. D.; Boehm, J. C.; Jakas, D. R.; Holden, K. G.; Hecht, S. M.; Gallagher, G.; Caranfa, M. J.; McCabe, F. L.; Faucette, L. F.; Johnson, R. K..; et al. Synthesis of water-soluble (aminoalkyl)camptothecin analogues: inhibition of topoisomerase I and antitumor activity. *J. Med. Chem.* **1991**, *34*, 98–107.
(13) Garcia-Carbonero, R.; Supko, J. G. Current perspectives on the clinical experience, pharmacology, and continued development of the camptothecins. *Clin. Cancer Res.* **2002**, *8*, 641–661.
(14) Giovanella, B. C.; Stehlin, J. S.; Hinz, H. R.; Kozielski, A. J.; Harris, N. J.; Vardeman, D. M. Preclinical evaluation of the anticancer activity and toxicity of 9-nitro-20(*S*)-camptothecin (rubitecan). *Int. J. Oncol.* **2002**, *20*, 81–88.
(15) Eckhardt, S. G.; Baker, S. D.; Eckardt, J. R.; Burke, T. G.; Warner, D. L.; Kuhn, J. G.; Rodriguez, G.; Fields, S.; Thurman, A.; Smith, L.; Rothenberg, M. L.; White, L.; Wissel, P.; Kunka, R.; DePee, S.; Littlefield, D.; Burris, H. A.; Von Hoff, D. D.; Rowinsky, E. K. Phase I and pharmacokinetic study of GI147211, a water-soluble camptothecin analogue, administered for five consecutive days every three weeks. *Clin. Cancer Res.* **1998**, *4*, 595–604.
(16) Minami, H.; Fujii, H.; Igarashi, T.; Itoh, K.; Tamanoi, K.; Oguma, T.; Sasaki, Y. Phase I and pharmacological study of a new camptothecin derivative, exatecan mesylate (DX-8951f), infused over 30 minutes every three weeks. *Clin. Cancer Res.* **2001**, *7*, 3056–3064.
(17) Burke, T. G. Chemistry of the camptothecins in the bloodstream. Drug stabilization and optimization of activity. *Ann. N.Y. Acad. Sci.* **1996**, *803*, 29–31.
(18) Bailly, C. Homocamptothecins: potent topoisomerase I inhibitors and promising anticancer drugs. *Crit. Rev. Oncol. Hematol.* **2003**, *45*, 91–108.
(19) Bom, D.; Curran, D. P.; Chavan, A. J.; Kruszewski, S.; Zimmer, S. G.; Fraley, K. A.; Burke, T. G. Novel A,B,E-ring-modified camptothecins displaying high lipophilicity and markedly improved human blood stabilities. *J. Med. Chem.* **1999**, *42*, 3018–3022.
(20) Lavergne, O.; Demarquay, D.; Bailly, C.; Lanco, C.; Rolland, A.; Huchet, M.; Coulomb, H.; Muller, N.; Baroggi, N.; Camara, J.; Le Breton, C.; Manginot, E.; Cazaux, J. B.; Bigg, D. C. Topoisomerase I-mediated antiproliferative activity of enantiomerically pure fluorinated homocamptothecins. *J. Med. Chem.* **2000**, *43*, 2285–2289.
(21) Lavergne, O.; Lesueur-Ginot, L.; Pla Rodas, F.; Kasprzyk, P. G.; Pommier, J.; Demarquay, D.; Prevost, G.; Ulibarri, G.; Rolland, A.; Schiano-Liberatore, A. M.; Harnett, J.; Pons, D.; Camara, J.; Bigg, D. C. Homocamptothecins: synthesis and antitumor activity of novel E-ring-modified camptothecin analogues. *J. Med. Chem.* **1998**, *41*, 5410–5419.
(22) Tangirala, R. S.; Antony, S.; Agama, K.; Pommier, Y.; Anderson, B. D.; Bevins, R.; Curran, D. P. Synthesis and biological assays of E-ring analogs of camptothecin and homocamptothecin. *Bioorg. Med. Chem.* **2006**, *14*, 6202–6212.
(23) Gelderblom, H.; Salazar, R.; Verweij, J.; Pentheroudakis, G.; de Jonge, M. J.; Devlin, M.; van Hooije, C.; Seguy, F.; Obach, R.; Prunonosa, J.; Principe, P.; Twelves, C. Phase I pharmacological and bioavailability study of oral diflomotecan (BN80915), a novel E-ring-modified camptothecin analogue in adults with solid tumors. *Clin. Cancer Res.* **2003**, *9*, 4101–4107.
(24) Demarquay, D.; Huchet, M.; Coulomb, H.; Lesueur-Ginot, L.; Lavergne, O.; Camara, J.; Kasprzyk, P. G.; Prevost, G.; Bigg, D. C. BN80927: a novel homocamptothecin that inhibits proliferation of human tumor cells in vitro and in vivo. *Cancer Res.* **2004**, *64*, 4942–4949.
(25) Hautefaye, P.; Cimetiere, B.; Pierre, A.; Leonce, S.; Hickman, J.; Laine, W.; Bailly, C.; Lavielle, G. Synthesis and pharmacological evaluation of novel non-lactone analogues of camptothecin. *Bioorg. Med. Chem. Lett.* **2003**, *13*, 2731–2735.
(26) Takagi, K.; Dexheimer, T. S.; Redon, C.; Sordet, O.; Agama, K.; Lavielle, G.; Pierre, A.; Bates, S. E.; Pommier, Y. Novel E-ring camptothecin keto analogues (S38809 and S39625) are stable, potent, and selective topoisomerase I inhibitors without being

substrates of drug efflux transporters. *Mol. Cancer Ther*. **2007**, *6*, 3229–3238.
(27) Pommier, Y. Camptothecins and topoisomerase I: a foot in the door. Targeting the genome beyond topoisomerase I with camptothecins and novel anticancer drugs: importance of DNA replication, repair and cell cycle checkpoints. *Curr. Med. Chem.: Anti-Cancer Agents* **2004**, *4*, 429–434.
(28) Pommier, Y.; Cushman, M. The indenoisoquinoline noncamptothecin topoisomerase I inhibitors: update and perspectives. *Mol. Cancer Ther*. **2009**, *8*, 1008–1014.
(29) Hsiang, Y. H.; Liu, L. F. Identification of mammalian DNA topoisomerase I as an intracellular target of the anticancer drug camptothecin. *Cancer Res*. **1988**, *48*, 1722–1726.
(30) Brangi, M.; Litman, T.; Ciotti, M.; Nishiyama, K.; Kohlhagen, G.; Takimoto, C.; Robey, R.; Pommier, Y.; Fojo, T.; Bates, S. E. Camptothecin resistance: role of the ATP-binding cassette (ABC), mitoxantrone-resistance half-transporter (MXR), and potential for glucuronidation in MXR-expressing cells. *Cancer Res*. **1999**, *59*, 5938–5946.
(31) Liao, Z.; Robey, R. W.; Guirouilh-Barbat, J.; To, K. K.; Polgar, O.; Bates, S. E.; Pommier, Y. Reduced expression of DNA topoisomerase I in SF295 human glioblastoma cells selected for resistance to homocamptothecin and diflomotecan. *Mol. Pharmacol*. **2008**, *73*, 490–497.
(32) Nakagawa, H.; Saito, H.; Ikegami, Y.; Aida-Hyugaji, S.; Sawada, S.; Ishikawa, T. Molecular modeling of new camptothecin analogues to circumvent ABCG2-mediated drug resistance in cancer. *Cancer Lett*. **2006**, *234*, 81–89.
(33) Fujimori, A.; Harker, W. G.; Kohlhagen, G.; Hoki, Y.; Pommier, Y. Mutation at the catalytic site of topoisomerase I in CEM/C2, a human leukemia cell line resistant to camptothecin. *Cancer Res*. **1995**, *55*, 1339–1346.
(34) Urasaki, Y.; Laco, G. S.; Pourquier, P.; Takebayashi, Y.; Kohlhagen, G.; Gioffre, C.; Zhang, H.; Chatterjee, D.; Pantazis, P.; Pommier, Y. Characterization of a novel topoisomerase I mutation from a camptothecin-resistant human prostate cancer cell line. *Cancer Res*. **2001**, *61*, 1964–1969.
(35) Meng, L. H.; Liao, Z. Y.; Pommier, Y. Non-camptothecin DNA topoisomerase I inhibitors in cancer therapy. *Curr. Top. Med. Chem*. **2003**, *3*, 305–320.
(36) Yamada, Y.; Tamura, T.; Yamamoto, N.; Shimoyama, T.; Ueda, Y.; Murakami, H.; Kusaba, H.; Kamiya, Y.; Saka, H.; Tanigawara, Y.; McGovren, J. P.; Natsumeda, Y. Phase I and pharmacokinetic study of edotecarin, a novel topoisomerase I inhibitor, administered once every 3 weeks in patients with solid tumors. *Cancer Chemother. Pharmacol*. **2006**, *58*, 173–182.
(37) Redinbo, M. R.; Stewart, L.; Kuhn, P.; Champoux, J. J.; Hol, W. G. Crystal structures of human topoisomerase I in covalent and noncovalent complexes with DNA. *Science* **1998**, *279*, 1504–1513.
(38) Staker, B. L.; Feese, M. D.; Cushman, M.; Pommier, Y.; Zembower, D.; Stewart, L.; Burgin, A. B. Structures of three classes of anticancer agents bound to the human topoisomerase I−DNA covalent complex. *J. Med. Chem*. **2005**, *48*, 2336–2345.
(39) Staker, B. L.; Hjerrild, K.; Feese, M. D.; Behnke, C. A.; Burgin, A. B., Jr.; Stewart, L. The mechanism of topoisomerase I poisoning by a camptothecin analog. *Proc. Natl. Acad. Sci. U.S.A*. **2002**, *99*, 15387–15392.
(40) Ioanoviciu, A.; Antony, S.; Pommier, Y.; Staker, B. L.; Stewart, L.; Cushman, M. Synthesis and mechanism of action studies of a series of norindenoisoquinoline topoisomerase I poisons reveal an inhibitor with a flipped orientation in the ternary DNA-enzyme-inhibitor complex as determined by X-ray crystallographic analysis. *J. Med. Chem*. **2005**, *48*, 4803–4814.
(41) Kolb, P.; Rosenbaum, D. M.; Irwin, J. J.; Fung, J. J.; Kobilka, B. K.; Shoichet, B. K. Structure-based discovery of beta2-adrenergic receptor ligands. *Proc. Natl. Acad. Sci. U.S.A*. **2009**, *106*, 6843–6848.
(42) Li, H.; Huang, J.; Chen, L.; Liu, X.; Chen, T.; Zhu, J.; Lu, W.; Shen, X.; Li, J.; Hilgenfeld, R.; Jiang, H. Identification of novel falcipain-2 inhibitors as potential antimalarial agents through structure-based virtual screening. *J. Med. Chem*. **2009**, *52*, 4936–4940.
(43) Shoichet, B. K. Virtual screening of chemical libraries. *Nature* **2004**, *432*, 862–865.
(44) Toshiya, K.; Shigeo, M.; Saburo, T. Stucture eludidation and synthesis of alkaloids isolated from fruits of *Evodia rutaecarpa*. *Agric. Biol. Chem*. **1978**, *42*, 1515–1519.
(45) Kametani, T.; Higa, T.; Fukumoto, K.; Koizumi, M. A one-step synthesis of evodiamine and rutecarpine. *Heterocycles* **1976**, *4*, 23–28.
(46) Whittaker, N. The synthesis of emetine and related compounds. Part VI. Improvements in the synthesis of 3-alkyl-1,3,4,6,7,11b-hexahydro-9,10-dimethoxybenzo[*a*]quinolizin-2-ones and 3-alkyl-1,2,3,4,6,7,12,12b-octahydroindolo[2,3-*a*]quinolizin-2-ones. Formation of some related diazabicyclo[3,3,1]nonanes. *J. Chem. Soc. C* **1969**, 85–89.
(47) Schöpf, C.; Steuer, H. Zur frage der biogenese des rutaecarpins und evodamins. Die synthese des rutaecarpins unter zellmöglichen bedingungen. *Justus Liebigs Ann. Chem*. **1947**, *558*, 124–36.
(48) Heilbron, I. M.; Kitchen, F. N.; Parkes, E. B.; Sutton, G. D. CCXCII.—Chemical reactivity and conjugation. Part II. The reactivity of the 2-methyl group in the 4-quinazolone series. *J. Chem. Soc., Trans*. **1925**, *127*, 2167–2175.
(49) Jiang, J.; Hu, C. Evodiamine: a novel anti-cancer alkaloid from *Evodia rutaecarpa*. *Molecules* **2009**, *14*, 1852–1859.
(50) Yoshizumi, M.; Houchi, H.; Ishimura, Y.; Hirose, M.; Kitagawa, T.; Tsuchiya, K.; Minakuchi, K.; Tamaki, T. Effect of evodiamine on catecholamine secretion from bovine adrenal medulla. *J. Med. Invest*. **1997**, *44*, 79–82.
(51) Lin, H.; Tsai, S. C.; Chen, J. J.; Chiao, Y. C.; Wang, S. W.; Wang, G. J.; Chen, C. F.; Wang, P. S. Effects of evodiamine on the secretion of testosterone in rat testicular interstitial cells. *Metabolism* **1999**, *48*, 1532–1535.
(52) Kobayashi, Y.; Nakano, Y.; Kizaki, M.; Hoshikuma, K.; Yokoo, Y.; Kamiya, T. Capsaicin-like anti-obese activities of evodiamine from fruits of *Evodia rutaecarpa*, a vanilloid receptor agonist. *Planta Med*. **2001**, *67*, 628–633.
(53) Chiou, W. F.; Sung, Y. J.; Liao, J. F.; Shum, A. Y.; Chen, C. F. Inhibitory effect of dehydroevodiamine and evodiamine on nitric oxide production in cultured murine macrophages. *J. Nat. Prod*. **1997**, *60*, 708–711.
(54) Kan, S. F.; Yu, C. H.; Pu, H. F.; Hsu, J. M.; Chen, M. J.; Wang, P. S. Anti-proliferative effects of evodiamine on human prostate cancer cell lines DU145 and PC3. *J. Cell. Biochem*. **2007**, *101*, 44–56.
(55) Yang, Z. G.; Chen, A. Q.; Liu, B. Antiproliferation and apoptosis induced by evodiamine in human colorectal carcinoma cells (COLO-205). *Chem. Biodiversity* **2009**, *6*, 924–933.
(56) Kobayashi, Y. The nociceptive and anti-nociceptive effects of evodiamine from fruits of *Evodia rutaecarpa* in mice. *Planta Med*. **2003**, *69*, 425–428.
(57) Chiou, W. F.; Chou, C. J.; Shum, A. Y.; Chen, C. F. The vasorelaxant effect of evodiamine in rat isolated mesenteric arteries: mode of action. *Eur. J. Pharmacol*. **1992**, *215*, 277–283.
(58) Tsai, T. H.; Lee, T. F.; Chen, C. F.; Wang, L. C. Thermoregulatory effects of alkaloids isolated from Wu-chu-yu in afebrile and febrile rats. *Pharmacol., Biochem. Behav*. **1995**, *50*, 293–298.
(59) Jones, G.; Willett, P.; Glen, R. C.; Leach, A. R.; Taylor, R. Development and validation of a genetic algorithm for flexible docking. *J. Mol. Biol*. **1997**, *267*, 727–748.
(60) Thomsen, R.; Christensen, M. H. MolDock: a new technique for high-accuracy molecular docking. *J. Med. Chem*. **2006**, *49*, 3315–3321.
(61) Morris, G. M.; Goodsell, D. S.; Halliday, R. S.; Huey, R.; Hart, W. E.; Belew, R. K.; Olson, A. J. Automated docking using a Lamarckian genetic algorithm and empirical binding free energy function. *J. Comput. Chem*. **1998**, *19*, 1639–1662.
(62) Huey, R.; Morris, G. M.; Olson, A. J.; Goodsell, D. S. A Semiempirical free energy force field with charge-based desolvation. *J. Comput. Chem*. **2007**, *28*, 1145–1152.